Effect of Extracellular Matrix Elements on the Transport of Paclitaxel through an Arterial Wall Tissue Mimic

Rachael W. Sirianni,[†] John Kremer,[‡] Ismail Guler,[‡] Yen-Lane Chen,[‡] Fred W. Keeley,[§] and W. Mark Saltzman*[,†]

Department of Biomedical Engineering, Yale University, New Haven, Connecticut 06511, Boston Scientific Corporation, Inc., Maple Grove, Minnesota 55311, and Research Institute, Hospital for Sick Children, Toronto, ON, Canada M5G 1X8

Received May 22, 2008; Revised Manuscript Received July 23, 2008

Paclitaxel (PTx) is reported to have an nonuniform steady-state concentration profile in the arterial wall. We utilized epifluorescence microscopy to make precise measurements of fluorescently-labeled PTx (F-PTx) distribution through an in vitro tissue mimic which contained varying concentrations of fibrin, elastin, soybean oil, palmitic acid, and solid glass beads. As little as 0.5 mg/mL of elastin in agarose produced a 50% drop in the measured diffusion coefficient, while as much as 10 mg/mL of fibrin in agarose was required for the same reduction in rate of transport. Because no reduction in the measured diffusion coefficient was observed for solubilized, extracted elastin or unassembled elastin-like polypeptides, the effect was specific to elastic fibers that closely resembled the native elastin network. Collectively, this work identifies a potential source for the high degree of partitioning observed for PTx in native tissue and further develops an in vitro technique for exploring complex tissue−drug interactions.

Introduction

Paclitaxel (PTx) is an antiproliferative agent that has been utilized in polymer coatings on vascular stents such as the TAXUS Express[2] Stent (Boston Scientific Corporation). TAXUS demonstrates improved long-term efficacy when compared to its bare metal counterparts,[1,2] and this improvement is believed to be due to the localized action of the drug PTx in reducing the response-to-injury process of neointimal hyperplasia at the implantation site.[3] Recent studies have reported nonuniform distribution of PTx following application of a labeled solution to arterial segments; the distribution of rapamycin, a similarly hydrophobic drug, was uniform.[4,5] PTx is known to bind to intracellular and extracellular tissue components, and it has been observed that PTx encounters tissue composition-dependent barriers to diffusion, whose source cannot be exclusively attributed to hydrophobic interactions.[4−9]

The rational design of safe and effective drug delivery devices relies on the ability to predict how the drug will interact with the body and distribute through the target tissue site. Traditional models designed to quantify drug distribution in tissue rely on measuring labeled drug distributions in whole organs or intact tissue. Typically, radiolabeled or fluorescently labeled drug is applied at some concentration via intravenous injection or directly to a tissue site. Following a period under which drug distributes through the tissue, the delivery site is extracted and analyzed for distribution between organ systems[10] or carefully sectioned to generate drug distribution profiles within particular tissue regions.[4,5,11,12] Whole-tissue techniques must assume that complex tissue structures are homogeneous across a given length scale. Such studies provide valuable information that often relates well to expected drug distributions in human subjects,[13] yet the ability of whole-tissue models to discern between numerous processes or subtle drug−tissue interactions is limited when the processes under consideration are smaller than the experimental length scale or concern single components of a multicomponent structure. Alternately, transport processes are measured under experimental conditions designed to isolate particular parameters such as protein binding constants or cellular permeability.[14,15] Experimental values are subsequently extrapolated to complex models that predict drug distributions in the body.[13,16−18] Modeling techniques based on empirically derived transport parameters are useful for generating predictions under specific experimental constraints, but such models can be limited in their applicability or suffer from assumptions that challenge the validity of their results.

There remains the need to understand drug distribution and interaction with delivery site from an intermediate perspective: to isolate the effects that individual components have on drug transport while retaining the ability to measure distributions of drug that are relevant to the complex interactions and networks or tissue components found in vivo. Such an analysis of drug distribution in a tissue-like material could only be performed where the diffusing medium contained some but not all of the complexity of native tissue. To this end, we have utilized a previously established technique[19,20] to study the transport of the PTx through tissue mimics containing isolated extracellular matrix (ECM) components relevant to the arterial wall.

It has been proposed that the unusual equilibrium distribution of PTx in tissue is due to nonhomogeneous distribution of binding sites[4,5] or structural parameters.[9] The nature of the proposed binding sites have not been determined conclusively. In this work, we have utilized quantitative methods to study the diffusion of PTx through gels containing a variety of tissue components relevant to the arterial wall, with the aim to begin unraveling the drug−tissue interactions that exist in intact tissue.

* To whom correspondence should be addressed. Malone Engineering Center, 55 Prospect Street, New Haven, CT 06511. Tel.: (203) 432-3900. Fax: (203) 432-0030. E-mail: mark.saltzman@yale.edu.
[†] Yale University.
[‡] Boston Scientific Corporation, Inc.
[§] Hospital for Sick Children.

10.1021/bm800571s CCC: $40.75
Published on Web 09/12/2008

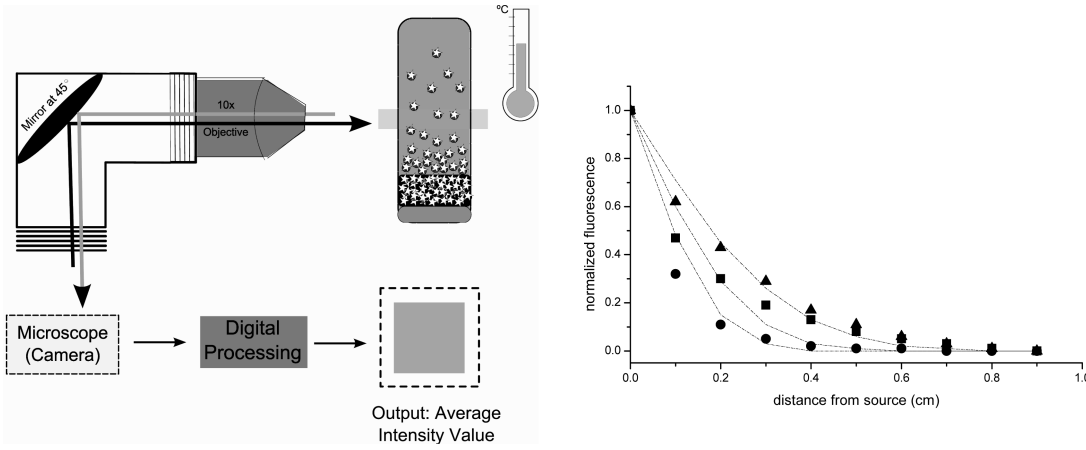

Figure 1. Experimental method for epifluorescence microscopy measurement of diffusion coefficients. A flat glass capillary tube (4 × 0.5 mm rectangular profile) was filled with agarose gel containing tissue components. Fluorescent drug in solution was applied at one end and the capillary tube sealed and maintained in a vertical orientation at a specified temperature. Images of the concentration gradient as it developed over time were captured with a camera; these intensity values were normalized and plotted as a function of time and distance. In the example on the right, measurements of F-PTx diffusing through 1% agarose gel were made at 3 (●), 5 (■), and 10 (▲) hrs; data fits, indicated by lines, generated a diffusion coefficient of 1.8×10^{-6} cm^2/sec.

Methods

Gel Construction. Oregon Green 488 Paclitaxel Conjugate (F-PTx, Invitrogen, Carlsbad CA) was chosen as a model for PTx due to its extensive use in the characterization of PTx binding in vivo;[21] although F-PTx is slightly more soluble in water than PTx, we do not expect altered solubility to affect diffusion measurements. Gel construction utilized a base of 1% (w/v) agarose powder (American Bioanalytical, Natick MA) in distilled water. The agarose solution was heated in a microwave until boiling, mixed well, heated for an additional 10 s, and added to additional components if necessary. For bovine serum albumin (BSA, Sigma, St. Louis MO) agarose gels, the agarose was maintained in a water bath (40 °C) just above its gelling temperature prior to addition of the protein. For all multicomponent gels, hot agarose was added to a vial containing the dispersant to achieve the desired concentration. The vial was held on vortex for 3−5 s and then the fluid was quickly drawn 3−4 inches into each capillary tube. The capillary tubes were allowed to cool for at least 10 min; for lyophilized bovine fibrin (Sigma), insoluble human aortic elastin (Sigma) and 75 μm glass bead (Sigma) gels, the capillary tube was flipped over several times as it cooled to prevent settling of the dispersant. After the gel had cooled, a small space (4 × 0.5 × 2 mm) was carved in the gel at the bottom of the tube with a 26-gauge needle tip. With the capillary tube inverted, ~10 μL of F-PTx solution (25−50 μg/mL Propanol) was added to fill the void space. The tube, fluid-side-up, was quickly pressed into Crit-O-Seal clay sealant (Krackeler Scientific Corporation, Albany NY), reinverted, and the outside of the tube was cleaned to remove any potential external fluorescent solution. Its vertical orientation was maintained in the dark for the duration of the experiment, at 21 °C, unless otherwise indicated.

Diffusion Measurements. A previously described microscope system[19,20] was utilized for these measurements (see figure 1). Briefly, a microscope (Nikon Diaphot TMD) was fitted with a small periscope with an attached 10× epifluorescence objective to reorient the fluorescent beam by 90°. A stage was constructed to allow precise vertical manipulation of the capillary tube in 1 mm increments, and the entire setup was enclosed in a Plexiglas surround. The temperature of the stage setup could be controlled by adjusting the temperature of air flowing through the Plexiglas surround. For each measurement, the capillary tube was centered in y axis (total width 4 mm) and the z axis (total depth 0.5 mm) by using the edge of the capillary as an aid for reference. The fluorescent signal was transmitted from the capillary tube, through the periscope, to a digital camera (SPOT Insight, Diagnostic Instruments, Sterling Heights MI), with input into a computer outfitted with image capture software (SPOT Advanced 4.6, Diagnostic Instruments). Images were gathered and saved as 1200 × 1600 jpg2 files. The file was then converted to jpg format and loaded into image analysis software (ImageJ, National Institute of Health). Average intensity for each image was calculated from the histogram.

Measurements were made over the course of approximately 10 h, with time points taken every 2−3 h at 1 mm increments along the x axis of the tube until the signal disappeared (5−10 mm, depending on the time point). Thus, each tube represented approximately 20−40 concentration measurements for which a diffusion coefficient was fitted. For fibrin particle gels at high concentration, multiple (3) passes were made along each tube length on the left, middle, and right sides to account for horizontal heterogeneity. Vertical heterogeneity or settling was not observed for any of the tubes tested, because the agarose gel concentration (1%) was high enough to create a solid gel. Microscope settings were maintained throughout each tube pass, although they may have varied between different tubes or at different times to keep the fluorescent intensity/concentration relationship within a linear working range.

Analysis. Assuming a highly concentrated source of drug with no resistance to transport at the fluid−gel interface, the following derivation of Fick's law is applicable[19]

$$\frac{C(x,t)}{C_0} = erfc\left(\frac{x}{2\sqrt{t \cdot D}}\right) \quad (1)$$

where $C(x,t)$ is the measured fluorescent intensity for each image, C_0 is the fluorescent intensity at the fluid−gel interface (measured for each time point), x is the distance from the fluid−gel interface (cm), t is the time of data collection (sec), and D is the diffusion coefficient (cm^2/sec) fitted to each data set. All data analysis was performed on values of normalized, relative concentrations. Measurements were made within a range where the fluorescent intensity was proportional to F-PTx concentration. Data fits were performed by adjusting the value for the diffusion coefficient until a minimum value for the mean square error was obtained with sensitivity to 10^{-7} cm^2/sec. For a measurement conducted over 10 h, with a resolution of 1 mm, the detection limit for this technique is estimated by (0.1 cm)^2/(10 hr·60·60 s/hr) ≈ 0.3×10^{-6} cm^2/sec (measurements are observed to plateau below this value). Data fits were conducted simultaneously for all time and distance points for the experiment, that is, $n = 1$ represents all measurements made for a single capillary tube.

Elastin Preparations. Insoluble human aorta elastin (purified as described by Starcher and Galione)[22] and solubilized bovine neck ligament elastin (α-elastin prepared by the method of Partridge, et al.)[23] were obtained from Sigma. Details of the recombinant expression and

Table 1. Accurate Measurements of the Diffusion Coefficient in Agarose Gel (1%) were Made under a Variety of Conditions[a]

temperature (°C)	diffusing molecule	hydro-	MW (kDa)	literature D ($cm^2/sec \times 10^6$)	measured D ($cm^2/sec \times 10^6$)	number of measurements
37	BSA-FITC	-philic	66	0.7[b]	0.87 ± 0.1	3
21	BSA-FITC	-philic	66	0.5[b]	0.55 ± 0.2	6
21	F-PTx	-phobic	1.3	2[c]	1.6 ± 0.1	18
21	fluorescein	-philic	0.38	5−10[c]	7.0 ± 1.1	3

[a] Error is expressed as standard deviation. [b] Experimentally determined value.[26] [c] Estimated by molecular weight.[27]

purification of the elastin-like polypeptide are published elsewhere.[24] Briefly, this polypeptide consists of exons 20−21−23−24−21−23−24−21−23−24−21−23−24 of human elastin. Exons 20 and 24 are typical hydrophobic domains of elastin and exons 21 and 23 are cross-linking domains, each containing two lysine residues that are available for cross-linking. This elastin-like polypeptide has been shown to mimic the self-assembly properties of native tropoelastin and can be cross-linked into an insoluble polymer with elastomeric properties similar to those of native insoluble elastin.[24,25]

Results

The accuracy of our experimental technique was verified by making measurements of the diffusion of a variety of compounds and comparing the experimentally obtained value to values published in literature. Hydrophobic and hydrophilic molecules were tested, as well as low and high molecular weight molecules (Table 1). In these experiments, the fitted diffusion coefficient was observed to be stable throughout the time course of each experiment (data not shown), that is, 10 h was a sufficient time period to characterize Fickian diffusion. Although the concentration profile was observed to deviate slightly from Fickian diffusion near the drug source−gel interface,[19] this deviation was small enough that the measurements produced by this technique were still accurate.

Control measurements were routinely conducted for F-PTx through agarose: a consistent value of the fitted diffusion coefficient of $1.6 \pm 0.3 \times 10^{-6}$ cm^2/s was observed. This value was not observed to change when measurements were made at different times during a period of several months or with varying capillary dimension; no significant decrease in the diffusion coefficient was observed for fluorescein dissolved in water versus propanol (data not shown). Thus, the technique utilized here provides accurate estimates of the diffusion coefficient.

Various materials were incorporated into the 1% agarose gel base. As the amount of nongel material was increased, the transport of F-PTx was observed to decrease, as reflected quantitatively in a decrease in the value of the fitted diffusion coefficient. Figure 2 illustrates this phenomenon for lyophilized fibrin particles suspended in agarose gel.

Diffusion coefficients were measured for F-PTx transport through a variety of gel composites: we examined gels containing insoluble elastin, BSA, fibrin, oil droplets, palmitic acid, or solid glass microspheres. The values obtained from these experiments are plotted together in Figure 3. Given the broad range of measured values, the diffusion coefficients are expressed as a function of nongel mass on a log scale. A similar trend was observed for elastin, BSA, fibrin, and oil droplets: the increasing presence of dispersed compounds resulted in a decrease in the measured diffusion coefficient. The magnitude of the drop in diffusion coefficient with mass of added material was highly dependent on the material under question, with hierarchy of material influence on transport for increasing effect: elastin > BSA > fibrin > lipid (Table 2). Glass microspheres and palmitic acid were not observed to affect the diffusion of F-PTx significantly, even when dispersed at very high concentrations (up to 400 mg/mL).

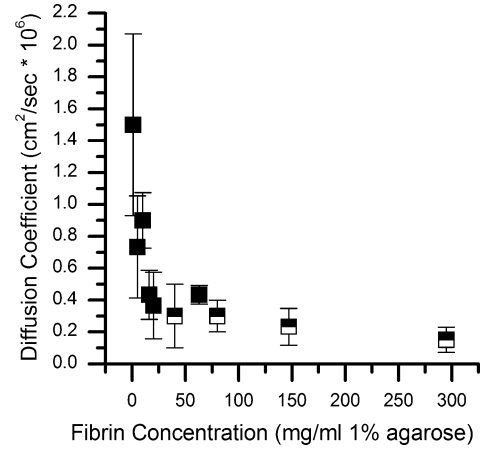

Figure 2. Measured effective diffusion coefficient for PTx decreases with increasing concentration of lyophilized fibrin in an agarose (1% w/v) base. Error is expressed as standard deviation of three samples and half-filled points indicate measurements near the detection limit for this technique.

The varying effects of dispersants on diffusion were also analyzed qualitatively by examining the unprocessed microscope images obtained during diffusion analysis. Note that because camera settings were altered between experiments in order to maintain the concentration/intensity relationship within a linear range, and because a whole-field (as opposed to two-photon or confocal) microscopy technique was utilized, the absolute fluorescence intensity was not comparable between unprocessed images. A summary of representative 1 mm wide microscope images is provided in Figure 4. Smooth, even gradients of image brightness were observed for all control gels, as demonstrated in Figure 4a. Several phenomena that are useful in qualitative interpretation of these figures were distinguished: (1) average intensity across the entire image, (2) diffusion of F-PTx through particles versus around particles, and (3) background versus particle concentration gradients.

For instance, F-PTx was observed to diffuse *through* fibrin particles (Figure 4d) in a time-dependent manner, in contrast to Figure 4c, where F-PTx diffuses *around* oil droplets; no F-PTx penetration into oil droplets was observed even after 24 h of incubation. Additionally, the relative difference between background and particle concentration varied for different materials: a weak background gradient of F-PTx in Agarose was observed in fibrin gels (Figure 4d), even though background fluorescence was almost absent from elastin composite gels of high concentration (figure 4e).

Because F-PTx diffusion was hindered most significantly by the presence of elastin, additional experiments were designed to learn more about the nature of the interaction between F-PTx and elastin. The human elastin precursor, tropoelastin is a 70 kDa protein, composed of 750−800 residues with alternating hydrophobic and cross-linking domains.[28] In vivo, tropoelastin

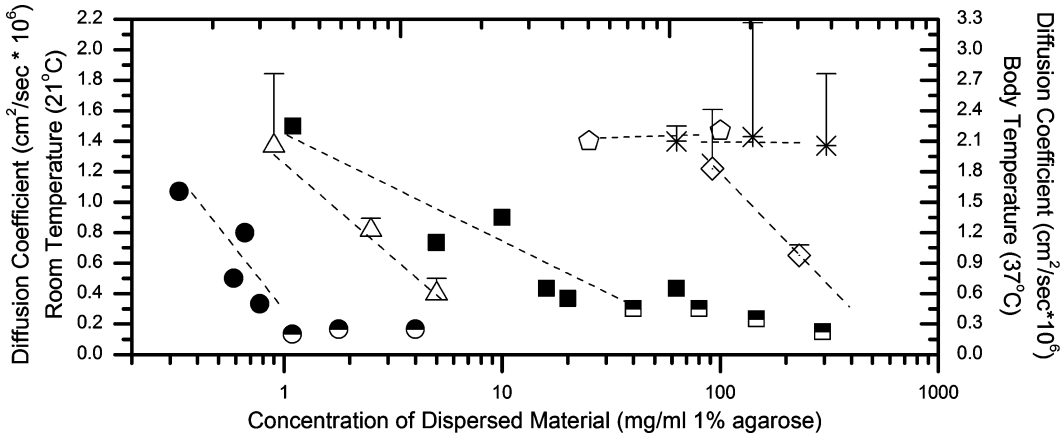

Figure 3. The estimated effective diffusion coefficient for PTx decreases with increasing concentration of (●) elastin, (Δ) BSA, (■) fibrin, (⬠) palmitic acid, (∗) glass beads, and (◇) oil droplets in an agarose base (1% w/v). Each point represents the average of three measurements. The measured diffusion coefficient for PTx through 1% agarose at room temperature (21 °C) was 1.6×10^{-6} cm^2/sec. The right axis contains values corrected to body temperature (37 °C) by the Stokes−Einstein relation for diffusion in water. The strength of effect on the measured diffusion coefficient ranges across several orders of magnitudes for different materials (note the log scale). Dashed lines are for illustrative purposes only. Error is expressed as standard deviation of three samples (two samples for oil droplets) and half-filled points indicate measurements near the detection limit for this technique.

Table 2. Concentration of Material in Agarose Gel at which the Effective Diffusion Coefficient of PTx Reaches 0.8×10^{-6} cm^2/sec Depends on the Material under Consideration[a]

material	mg/mL
elastin	0.5
BSA	2.5
fibrin	10
soybean oil	150
palmitic acid	>200
glass beads	>200

[a] Control value of PTx through 1% agarose is equal to 1.6×10^{-6} cm^2/sec.

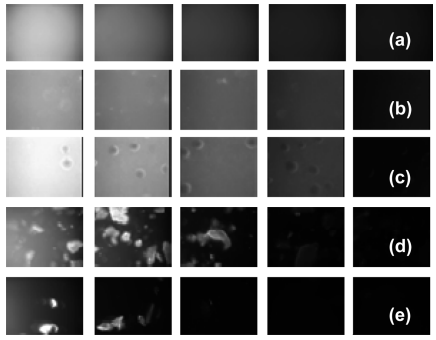

Figure 4. Unprocessed data in the form of microscope images reveal interesting differences between the tissue mimics tested here. F-PTx sources is located on the left with zero concentration sink on the right. In 1% agarose, the (a) control gel contains no dispersant and (b−e) contain BSA, soybean oil, fibrin particles, and elastin particles. For future quantitative analysis, all fluorescent intensities were normalized to the left-most image from each pass along the capillary tube.

cross-links, forming a polymeric product that is highly insoluble. Purification of polymeric elastin generally consists of extraction procedures that remove all other contaminating proteins, leaving pure elastin as an insoluble residue. This extraction technique is believed to minimize peptide cleavage and thus preserve the structure of native elastin fibers.[22] The insoluble elastin product may be further processed by chemical hydrolysis, yielding a solubilized elastin product consisting of large polypeptide fragments of elastin.[29] The elastin precursor, tropoelastin, may also be produced in recombinant form. Recombinant human elastin-like polypeptides are soluble in water and will self-assemble upon heating to form an elastin network that can be cross-linked to produce biomaterials that possess properties similar to native elastin.[24,25]

We examined diffusion in gels containing three elastin products (purified insoluble with preserved structure, EP-I; insoluble elastin that has been solubilized by partial proteolysis, EP-S; and recombinant human elastin-like polypeptides, EP-R). EP-I is expected to most closely mimic native insoluble elastin structure. EP-S is expected to have preserved cross-links with shortened chain length, while EP-R is an unassembled, shortened form of native elastin. Diffusion studies revealed that, for the concentrations tested here, EP-S and EP-R did not affect diffusion of F-PTx to the same extent as EP-I (Figure 5).

Discussion

Our technique yielded an estimate of the diffusion coefficient for F-PTx in agarose gel of 1.6×10^{-6} cm^2/sec at 21 °C. Based on its molecular weight, the diffusion coefficient of F-PTx is 2×10^{-6} cm^2/sec for free diffusion in solution.[27] At a low concentration of agarose (1%), the diffusion of small molecular weight agents is not expected to be hindered.[30] The stability of the diffusion coefficient measurement over the time course of these experiments, and through different batches of reagent, indicates that the fluorescent tag is stably attached to the PTx molecule (breakdown of the fluorescent label attachment would be reflected in an increased diffusion coefficient). The control diffusion coefficient values for fluorescein and BSA-FITC with varying gel concentration and temperature are within range of literature values, confirming that this technique is accurate under the conditions tested here.

The measured diffusion coefficient for F-PTx in this system is similar to diffusion coefficients reported in vivo. The PTx diffusion coefficient is reported to be on the order of 10^{-6} cm^2/sec when transport occurs in a direction parallel to the arterial wall tissue layers; the same measurement made for transport occurring perpendicular to tissue layers results in a diffusion coefficient that is significantly less, on the order of 10^{-10} cm^2/sec.[4] A longitudinal measurement made for transport occurring parallel to tissue layers allows drug to follow the path of least resistance, which is comparable to our experimental setup. Because all materials tested in this study yielded diffusion coefficients of approximately 10^{-6} cm^2/sec, we have further

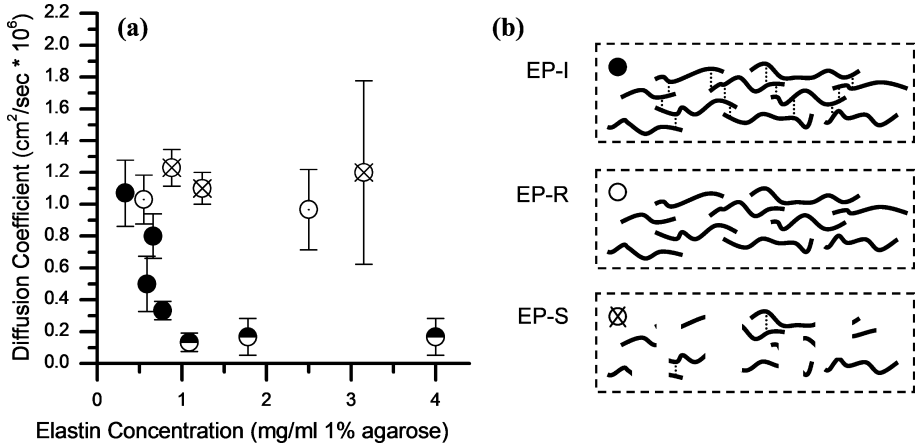

Figure 5. F-PTx diffusion is reduced in the presence of elastin. (a) The interaction of F-PTx with elastin is specific to purified, insoluble elastin EP-I (●). Soluble, recombinant human elastin-like polypeptide EP-R (○) and soluble, hydrolyzed extracted elastin EP-S (⊗) did not affect the measured diffusion coefficient to the same extent. Error expressed as standard deviation of three samples, and half-filled points indicate measurements taken near the detection limit for this technique. (b) Illustrative structures for EP-I, EP-S, and EP-R. EP-I is expected to have preserved cross-links, whereas EP-R consists of unassembled elastin-like polypeptides. EP-S is a degraded product.

confirmation that these measured values are in accordance with expected values for diffusion in tissue. Dispersing high concentrations of glass particles in the gel did not appreciably impact transport for the range of concentrations studied here, indicating that that any observed reduction in transport of F-PTx is not a result of decreased volume fraction or the resulting increase in tortousity.

We observed that the transport of a PTx analog can be significantly influenced by molecules that are present in biological tissues and fluids Increasing concentration of biological molecule resulted in a stronger reduction in the rate of transport of F-PTx through the tissue mimic to values approaching 3×10^{-7} cm^2/sec (given that fluorescence intensity was averaged over 1 mm segments, which often included the high intensity source, diffusion coefficients significantly below this value cannot be measured). It is evident from our results that the extent to which transport is slowed (reflected by a decrease in the measured diffusion coefficient) is highly dependent on the material added to the gel environment. For example, to produce a 50% decrease in the effective diffusion coefficient from 1.6×10^{-6} cm^2/sec for agarose to 0.8×10^{-6} cm^2/sec for agarose-material requires ~150 mg of soybean oil versus 10 mg of fibrin particles or 0.5 mg of elastin particles per mL of agarose gel. In elastin−agarose composite gels, F-PTx was almost completely absent from the agarose phase yet fluoresced brightly in regions containing extracted elastin fibers; this degree of partitioning into ECM material was not observed for any other material tested in these experiments. We conclude that insoluble, polymeric elastin fibers readily bind large quantities of F-PTx, resulting in significantly reduced transport even at very low volume fractions of elastin.

Our results suggest that small quantities of elastin will provide a significant barrier to transport, whereas the presence of other ECM materials such as fibrin or lipid buildup will have a minimal effect on the transport of PTx. Additionally, small changes in the relative amount of elastin at different locations throughout the arterial wall are expected to result a nonuniform steady-state concentration profile, such that PTx preferentially distributes into regions of high elastin content. Thus, we have identified an additional feature of PTx transport through this analysis: the location and content of elastin fibers are expected to have a critical effect on the distribution of PTx in native tissue networks.

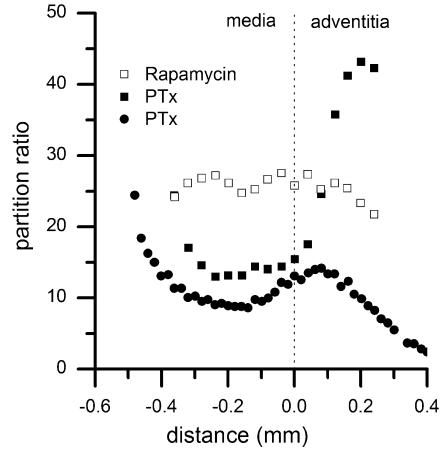

Figure 6. Reports on the distribution of PTx in intact tissue observed that the equilibrium concentration profile demonstrates a high degree of partitioning of PTx into tissue that is similar in overall amount to rapamycin but not in distribution. In Creel, et al. (●), high partitioning is observed near the intima and between the media and the adventitia (calf common carotid artery).[4] In Levin, et al. (■), high partitioning is observed near the intima and in the adventitia (calf internal carotid artery).[5] The distribution of rapamycin (□) through the arterial wall is relatively homogeneous in comparison.[1,5]

The distribution of elastin fibers in many tissue types is relatively homogeneous (e.g., skin or lungs), however, in blood vessels, discrete elastic lamina form concentric layers in the vessel wall. The distribution of labeled PTx through arterial tissue samples has been measured,[4,5] and results from these studies suggest that at steady-state, the concentration of PTx is maximal at the intima and drops with increasing tissue depth; a region of high partitioning occurs near the boundary between the media and adventitia, where the elastin network is expected to be at a high concentration. The drugs PTx and rapamycin are characterized by similar solubility and molecular weight. Based on this chemical similarity, PTx and rapamycin would be expected to have similar distribution profiles in tissue, yet, the rapamycin profile is spatially homogeneous and the PTx profile is not (Figure 6). Both PTx and rapamycin accumulate in tissue to a greater extent than dextran, a water soluble molecule, yet PTx distributes preferentially to certain tissue regions. While there is some disagreement on the exact equilibrium profile that is reached for PTx (it is possible that there are differences in the composition of vessels obtained from

different tissue sites), there is agreement that the atypical concentration profile for PTx is most likely a result of binding to specific tissue elements, and that the effect is distinct from other drugs tested.[4,5]

We examined different elastin preparations with the aim to identify features of the elastin network necessary to slow transport of PTx. At the concentrations of material tested here (0−4 mg material per mL agarose), intact, insoluble, polymeric elastin fibers were necessary to have an effect on transport. Partially hydrolyzed, solubilized elastin (EP-S) and unassembled, soluble, recombinant elastin-like polypeptides (EP-R) did not have the same effect on transport. EP-S and EP-R are of shorter chain length than EP-I, and lower molecular weight chains might have the potential to diffuse through dilute agarose gel. Diffusion of elastin or polypeptide chains could mask some (although not all) of a PTx/binding effect because the bound PTx would not longer be immobilized. However, given that the mean molecular weight of these products are still relatively high ($\geq$30 kDa, compared to $\sim$1 kDa for F-PTx), we anticipate that diffusion of elastin or polypeptide chains would be minimal, if present at all. Additionally, while native elastic fibers contain other protein components such as fibrillins, it is unlikely that any of these proteins would be present in significant quantities given the extraction technique.[22,29] Macromolecular contaminants are not expected to influence the measurements made here. These results suggest two possible features of dispersed material that could be necessary for the elastin effect: (1) localized, highly concentrated regions of protein or (2) full length, cross-linked elastin.

With regards to the first hypothesis, it could be possible that the high concentration of elastin material present in the intact, insoluble lyophilized particles provides a nonspecific driving force for F-PTx to partition into regions of lower water content. While this idea of a nonspecific interaction is plausible, it should be noted that we do not see this effect in fibrin particles or oil droplets, two materials that both provide a nonaqueous environment for potential partitioning. In the case of the oil, it may be that the water−oil interface presents a sufficient barrier to diffusion that prohibits partitioning within the time frame studied here; yet, fibrin particles would be expected to have an equally strong influence of F-PTx transport if partitioning due to hydrophobicity is the only process occurring and the effect of fibrin particles in gel on the diffusion coefficient was significantly lower than the effect of elastin. We have also tested gels dispersed with lyophilized polymer microspheres made of high concentrations of alginate, and partitioning has not been observed (data not shown). Furthermore, the partitioning hypothesis is inconsistent with in vivo data demonstrating different steady-state concentration profiles for rapamycin and PTx.[5] The fact that a strong effect on transport was only observed in the insoluble elastin particle gels and at relatively low concentration of elastin suggests that assembled elastin possesses binding sites for PTx that are not available on the other materials tested.

To address the second hypotheses, it is necessary to understand the structure of native elastin. The elastin precursor, tropoelastin, exists as a protein with alternating hydrophobic and cross-linking domains. Under the right conditions, tropoelastin will self-assemble to form a cross-linked elastin network in a process known as coacervation: as the solution temperature rises, the interaction of hydrophobic domains brings cross-linking domains within proximity to form covalent bonds. Lysine residues present on monomeric tropoelastin are converted to desmosine and other cross-links. The resulting network of cross-linked elastin retains the alternating hydrophobic/cross-linking sequence, but the majority of the lysines in cross-linking domains are used in the cross-linking process. ^{13}C NMR studies of recombinant elastin peptides demonstrate cooperativity between different regions within the tropoelastin, whereby substitutions to the cross-linking domain resulted in unexpected changes to the hydrophobic domains.[31] EP-R is expected to retain a highly positive charge as a result of the presence of lysine residues in the cross-linking domains whereas cross-linking present in EP-I or EP-S could affect the potential for PTx binding by altering the accessibility of certain peptide domains. Finally, the shorter chain length of EP-S could result in fewer conformational possibilities, thus reducing the potential for PTx to bind. Taken collectively, these observations suggest that F-PTx interacts preferentially with intact, polymeric elastin fibers that are similar to the elastin network found in vivo.

We have identified differences in F-PTx transport in protein and lipid loaded gels which suggest mechanisms for PTx transport through intact tissue of the arterial wall. We observed that elastin has a substantial influence on the transport parameters measured with an epifluorescence microscopy technique, and also that we can use this information to better understand ex vivo results that suggest a nonuniform distribution of PTx in tissue. While the exact mechanism underlying the PTx−elastin interaction remains to be determined, observations from this work support a strong interaction of PTx with dense regions of cross-linked insoluble elastin.

Conclusion

Epifluorescence microscopy was used to measure effective diffusion coefficients for transport of a variety of fluorescently labeled molecules through agarose-based tissue mimics. We observed that proteins and lipids dispersed in agarose gel resulted in a significant reduction in the measured diffusion coefficient for fluorescently labeled PTx when compared to pure agarose gels, and this effect was not due to an increase in tortuosity. Extracted, insoluble elastin fibers had the greatest impact on transport observed for any of the molecules tested here, with concentrations in the range of 0.5 mg/mL, resulting in a 50% reduction in the measured diffusion coefficient; a similar reduction in the measured diffusion coefficient was not observed for solubilized elastin fibers or for recombinant elastin-like polypeptides, indicating that the interaction of F-PTx with elastin is specific to insoluble elastin networks that resemble the intact elastin fibers found in vivo. The strong reduction in transport rate observed for the in vitro tissue mimics containing purified insoluble elastin when compared to both agarose controls as well as other proteins and lipid dispersed gels may explain the unusual distribution of PTx observed in intact tissue. The results obtained from these diffusion studies are relevant both in understanding the fate of PTx within the body and in making predictions relevant to ex vivo tissue studies.

References and Notes

(1) Stone, G. W.; Ellis, S. G.; Cannon, L.; Mann, J. T.; Greenberg, J. D.; Spriggs, D.; O'Shaughnessy, C. D.; DeMaio, S.; Hall, P.; Popma, J. J.; Koglin, J.; Russell, M. E. *JAMA, J. Am. Med. Assoc.* **2005**, *294*, 1215–1223.

(2) Colombo, A.; Drzewiecki, J.; Banning, A.; Grube, E.; Hauptmann, K.; Silber, S.; Dudek, D.; Fort, S.; Schiele, F.; Zmudka, K.; Guagliumi, G.; Russell, M. E. *Circulation* **2003**, *108*, 788–794.

(3) Axel, D. I.; Kunert, W.; Gogglemann, C.; Oberhoff, M.; Herdeg, C.; Ku?ttner, A.; Wild, D. H.; Brehm, B. R.; Riessen, R.; Koveker, G.; Karsch, K. R. *Circulation* **1997**, *96*, 636–645.

(4) Creel, C. J.; Lovich, M. A.; Edelman, E. R. *Circ. Res.* **2000**, *86*, 879–884.

(5) Levin, A. D.; Vukmirovic, N.; Hwang, C. W.; Edelman, E. R. *Proc. Natl. Acad. Sci. U.S.A.* **2004**, *101*, 9463–9467.
(6) Hwang, C. W.; Edelman, E. R. *Circ. Res.* **2002**, *90*, 826–832.
(7) Manfred, J. J.; Parness, J.; Horwitz, S. B. *J. Cell Biol.* **1982**, *94*, 688–696.
(8) Lovich, M. A.; Creel, C.; Hong, K.; Hwang, C. W.; Edelman, E. R. *J. Pharm. Sci.* **2001**, *90*, 1324–1335.
(9) Au, J. S.; Jang, S. H.; Zheng, J.; Chen, C. T.; Song, S.; Hu, L.; Wientjes, M. G. *J. Controlled Release* **2001**, *74*, 31–46.
(10) Sparreboom, A.; Van Tellingen, O.; Nooijen, W. J.; Beijnen, J. H. *Anti-Cancer Drugs* **1996**, *7*, 78–86.
(11) Touitou, E.; Meidan, V. M.; Horwitz, E. *J. Controlled Release* **1998**, *56*, 7–21.
(12) Tao, L.; Nicholson, C. *Neuroscience* **1996**, *75*, 839–847.
(13) Obach, R. S.; Baxter, J. G.; Liston, T. E.; Silber, B. M.; Jones, B. C.; Macintyre, F.; Rance, D. J.; Wastall, P. *J. Pharmacol. Exp. Ther.* **1997**, *283*, 46–58.
(14) Sonnichsen, D. S.; Relling, M. V. *Clin. Pharmacokinet.* **1994**, *27*, 256–269.
(15) Artursson, P.; Karlsson, J. *Biochem. Biophys. Res. Commun.* **1991**, *175*, 880–885.
(16) Germani, M.; Crivori, P.; Rocchetti, M.; Burton, P. S.; Wilson, A. G. E.; Smith, M. E.; Poggesi, I. *Eur. J. Pharm. Sci.* **2007**, *31*, 190–201.
(17) Grass, G. M. *Adv. Drug Delivery Rev.* **1997**, *23*, 199–219.
(18) Balakrishnan, B.; Tzafriri, A. R.; Seifert, P.; Groothuis, A.; Rogers, C.; Edelman, B. R. *Circulation* **2005**, *111*, 2958–2965.
(19) Radomsky, M. L.; Whaley, K. J.; Cone, R. A.; Saltzman, W. M. *Biomaterials* **1990**, *11*, 619–624.
(20) Saltzman, W. M.; Radomsky, M. L.; Whaley, K. J.; Cone, R. A. *Biophys. J.* **1994**, *66*, 508–515.
(21) Fernando Diaz, J.; Strobe, R.; Engelborghs, Y.; Souto, A. A.; Andreu, J. M. *J. Biol. Chem.* **2000**, *275*, 26265–26276.
(22) Starcher, B. C.; Galione, M. J. *Anal. Biochem.* **1976**, *74*, 441–447.
(23) Partridge, S. M.; D., H. F.; Adair, G. S. *Biochem. J.* **1955**, *61*, 11–21.
(24) Miao, M.; Bellingham, C. M.; Stahl, R. J.; Sitarz, E. E.; Lane, C. J.; Keeley, F. W. *J. Biol. Chem.* **2003**, *278*, 48553–48562.
(25) Bellingham, C. M.; Lillie, M. A.; Gosline, J. M.; Wright, G. M.; Starcher, B. C.; Bailey, A. J.; Woodhouse, K. A.; Keeley, F. W. *Biopolymers* **2003**, *70*, 445–455.
(26) Liang, S.; Xu, J.; Weng, L.; Dai, H.; Zhang, X.; Zhang, L. *J. Controlled Release* **2006**, *115*, 189–196.
(27) Saltzman, W. M. *Drug Delivery: Engineering Principles for Drug Therapy*; Oxford University Press: New York, 2001; p 371.
(28) Debelle, L.; Tamburro, A. M. *Int. J. Biochem. Cell Biol.* **1999**, *31*, 261–272.
(29) Partridge, S. M.; Davis, H. F. *Biochem. J.* **1955**, *61*, 21–30.
(30) Slade, A. L.; Cremers, A. E.; Thomas, H. C. *J. Phys. Chem.* **1966**, *70*, 2840–2844.
(31) Kumashiro, K. K.; Ho, J. P.; Niemczura, W. P.; Keeley, F. W. *J. Biol. Chem.* **2006**, *281*, 23757–23765.

BM800571S